Design and Implementation of Battery Charger with Zero-Voltage-Switching Resonant Converter for Photovoltaic Arrays

*Ying-Chun Chuang **Hung-Shiang Chuang *Yu-Lung Ke, Member, IEEE

*Department of Electrical Engineering
Kun Shan University
Tainan, Taiwan, R.O.C.

** Department of Automation Engineering
Kao Yuan University
Kaohsiung, Taiwan, R.O.C.

Abstract -The high-frequency resonant converter has numerous well-known advantages over traditional hard switching converters. The most important advantage is that it offers a lower switching loss and a higher power density. Additionally, the soft-switching current waveform characterizes lower electromagnetic interference (EMI). This study presents the circuit configuration with the least components to realize a highly efficient solar energy battery charger with a zero-voltage-switching resonant converter. The optimal values of the resonant components are determined by applying the characteristic curve and the electric functions derived from the circuit configuration. The experiment demonstrates the switching on and off of the main switch in a solar energy battery charger with a zero-voltage-switching resonant converter, whose switches are all operated using zero-voltage switching. The circuit efficiency in the overall charging process exceeds 80%.

Keywords- Photovoltaic array, battery charger, resonant converter, zero-voltage-switching (ZVS).

I. INTRODUCTION

Because the issue of environmental protection resumes and the price of petroleum rises rapidly, the attempt to seek for alternative energy sources is a goal that would take universal efforts throughout the world. Among them, the solar energy is abundant, continuous supplying and pollution-free; hence, solar energy research has drawn a lot of attention. Taiwan is located in the subtropical zone, with lots of sunlight and long sunny days. Therefore, solar energy should be the most prominent candidate for green energy [1].

A high performance battery charger is necessary in a photovoltaic array and the charging mode markedly affects battery life and capacity. The traditional battery charger, which extracts power from an ac-line source, requires a thyristor AC/DC converter rectifier, with an equivalent series resistance, to control the power flow to charge the battery system. Such a charging circuit necessarily draws a high ripple charging current, which is notorious for very low efficiency and is associated with a large volume. Accordingly, as concern about the quality of a charger grows, a high performance charging circuit for reducing ripple and extending battery life becomes important in designing battery storage systems. Several charging circuits have been proposed to overcome the disadvantages of the traditional battery charger. The linear power supply is the simplest. A 60Hz transformer is required to deliver the output within the desired voltage range. However, the linear power supply is operated at the line frequency which is large both in size and weight. Besides, the system conversion efficiency is very low because the power switch operates in the active region. Hence, when a higher power is required, the use of an over-weighted and oversized line-frequency transformer makes this approach impracticable.

The photovoltaic arrays are not cheap. In order to minimize the losses, it is essential not to waste energy in the conversion process. In relation to the power electronics and associated control schemes, the main requirement is to ensure that the charging system is efficient. Therefore, topologies with high switching frequencies were used to reduce the charging current ripple and extend battery life. However, as the switching frequency increases further, switching losses and EMI noise arise [2-6]. To solve this problem, the switching frequency is increased by reducing the switching losses through a zero-voltage-switching (ZVS) resonant converter. The high-frequency operation of conventional converter topologies depends on a considerable reduction in switching losses to minimize size and weight. In switch-mode topologies, controllable switches are operated under hard-switching conditions, resulting in increased switching losses, switching noise, and EMI. In an attempt to overcome these shortcomings, much effort has been made to find a less expensive circuit topology and control scheme of the charging circuit, so as to offer a competitive price in the consumer market. This work considers the application of ZVS technique to a battery charger to minimize switching losses and switching noise and to reduce high-frequency EMI. In the developed approach, a resonant tank is inserted between the photovoltaic arrays and the battery. With the ZVS topology, a charger with high efficiency can be achieved without an additional power switch or sophisticated control circuit.

II. CIRCUIT DESCRIPTION

The block diagram of the proposed system is shown in

1-4244-0336-7/06/$20.00 ©2006 IEEE.

Fig. 1. The photovoltaic arrays output is filtered by inductor L_f and capacitor C_f and fed to the input of the DC-DC converter. The photovoltaic arrays output is converted to a high frequency voltage source using a DC-DC converter. The charging voltage at the output of the DC-DC stage can be regulated by varying the switching frequency of the control circuit. The most efficient method of controlling the charging current (and charging voltage) is to incorporate pulse-width-modulated (PWM) control within the charger circuit. However, PWM rectangular voltage and current waveforms cause turn-on and turn-off losses that limit the operating frequency. The key idea is to use a ZVS resonant-switch converter.

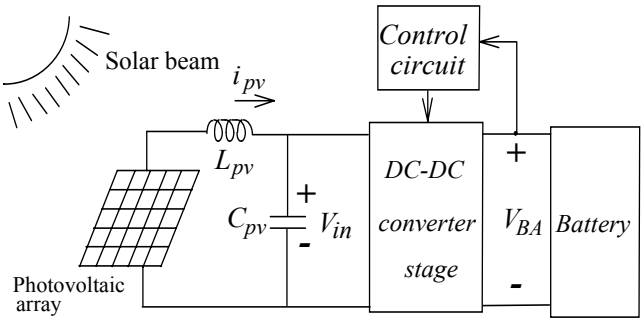

Fig. 1 Block diagram of the charging circuit for photovoltaic arrays

Figure 2 depicts the main circuit structure of the charging circuit with ZVS resonant-switch converter for a battery charger. It differs from a conventional PWM converter in that it has an additional resonant tank that comprises a resonant inductor L_r, a resonant capacitor C_r, and a freewheeling diode D_m. The internal switch capacitance C_j is added with the capacitor C_r, and it is affects the resonant frequency only, thereby contributing no power dissipation in the power switch. The resonant inductor L_r is connected in series to power switch Q to limit di/dt of the power switch, and the resonant capacitor C_r is installed as an auxiliary energy transfer element. The components L_r and C_r constitute a series resonant circuit whose oscillation is initiated by turning off the power switch Q. The power switch must be turned on only at zero voltage. Otherwise, the energy stored in C_r can be dissipated in the power switch. To avoid this situation, the antiparallel diode D_r must conduct before turning on the power switch. In this configuration, since the output voltage v_x is pulsed, a low pass filter composed of an inductor L_f and a capacitor C_f is necessary between the ZVS converter and the battery to make the ZVS charging circuit output current continuous. To simplify the analysis, the output filter inductance L_f is assumed to be sufficiently large to be regarded as an ideal dc current source I_o during a high-frequency resonant cycle.

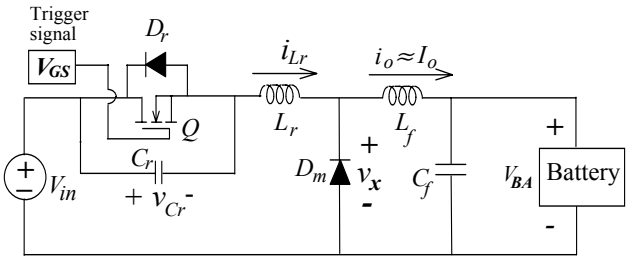

Fig.2 Circuit diagram of a zero-voltage-switching resonant converter for battery charger

Figure 3 plots the key waveforms of the buck ZVS converter. In one switching cycle, the circuit operation can be divided into four modes.

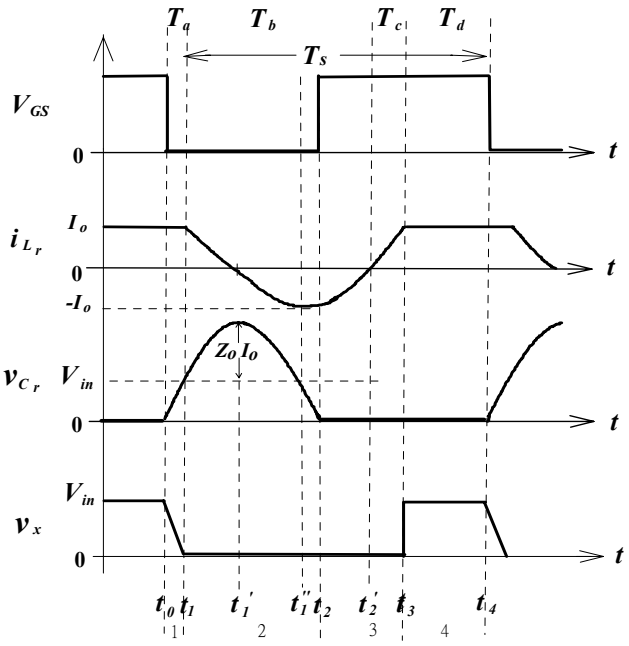

Fig. 3 Key waveforms of the proposed charging circuit with ZVS resonant converter

III. ANALYSIS OF THE PROPOSED CONVERTER

The analysis of this system is carried out under the following assumptions:

(i) Switching elements of the converter are ideal, i.e. forward voltage drops in on-state resistances of the switch are neglected.
(ii) The equivalent series resistance of the capacitance and stray capacitances are neglected.
(iii) Passive components are assumed to be linear, time-invariant and frequency-independent.

In a high-frequency switching cycle, the charging circuit with ZVS resonant-switch converter operates in the four following modes.

Mode 1: (between t_0 and t_1)

Prior to t_0, the power switch Q is on, and conducts a drain current that equals the output current I_O, and the freewheeling diode D_m is off. At the instant t_0, the power switch Q is turned off. The current through the resonant inductor L_r does not change instantaneously, so the current is diverted around the power switch through the resonant

capacitor C_r. The equivalent circuit of this operating mode is depicted in Fig. 4. The current of the resonant inductor equals the output current I_O and the capacitor voltage v_{Cr}, which is given by

$$v_{Cr}(t) = \frac{I_o}{C_r} t \tag{1}$$

Voltage across freewheeling diode D_m is determined by

$$v_x(t) = V_{in} - v_{c_r}(t) = V_{in} - \frac{I_o}{C_r} t \tag{2}$$

The voltage v_x declines to zero at time t_1 when D_m is turned on by soft-switching. The constant output current linearly increases the voltage across the resonant capacitor until the input voltage is reached. The time interval T_a is

$$T_a = \frac{V_{in} C_r}{I_o} \tag{3}$$

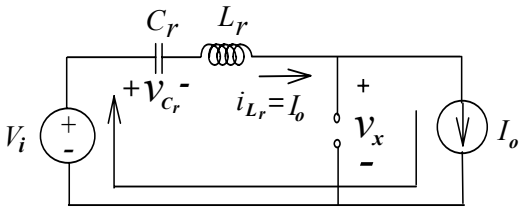

Fig. 4 Equivalent circuit for operating mode 1

Mode 2: (between t_1 and t_2)

After t_1, the freewheeling diode D_m becomes forward-biased, and C_r and L_r resonate. Fig. 5 shows the equivalent circuit.

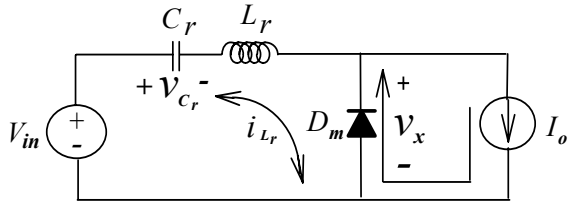

Fig. 5 Equivalent circuit for operating mode 2

The instantaneous voltage across C_r and the resonant inductor current can be evaluated, respectively

$$v_{C_r}(t) = Z_o I_o \sin \omega_o (t - t_1) + V_{in} \tag{4}$$

$$i_{L_r}(t) = I_o \cos[\omega_o (t - t_1)] \tag{5}$$

where the resonant angular frequency $\omega_o = \frac{1}{\sqrt{L_r C_r}}$ and the characteristics impedance $Z_o = \sqrt{\frac{L_r}{C_r}}$.

The voltage across the freewheeling diode D_m in Fig. 5 can then be given as

$$v_x(t) = 0 \tag{6}$$

The freewheeling diode current wave shape follows a cosine function during this interval, and equals I_O minus i_{Lr}(t). The resonant time is determined by solving the resonant capacitor voltage equation under the zero voltage condition.

$$(t_2 - t_1) = \frac{1}{\omega_o}\left[\sin^{-1}\left(\frac{V_{in}}{Z_o I_o}\right) + \pi\right] \tag{7}$$

Then,

$$T_b = \frac{1}{\omega_o}\left[\sin^{-1}\left(\frac{V_{in}}{Z_o I_o}\right) + \pi\right] \tag{8}$$

The above equation indicates that load current I_O is sufficiently large that $Z_O I_O > V_{in}$. Otherwise, the voltage of the power switch would not return to zero naturally, and the power switch has to be turned on at a nonzero voltage, causing turn-on losses. This interval ends at t_2 when v_{Cr} decreases to zero and the antiparallel diode D_r begins to conduct.

Mode 3: (between $t_2$and t_3)

After diode D_r is turned on, the voltage across C_r is clamped at zero. The turn-on signal of power switch Q is applied when the antiparallel diode is conducting to achieve ZVS. The equivalent circuit of this operating mode is sketched in Fig. 6. During this interval, the inductor current i_{Lr} is expressed as

$$i_{L_r}(t) = \frac{V_{in}}{L_r}(t - t_2) + I_o \cos[\omega_o (t_2 - t_1)] \tag{9}$$

The resonant inductor current $i_{Lr}(t)$ is linearly returned from the negative peak of I_O to its positive value I_O. Consequently, $i_{Lr}(t)$ increases linearly and the freewheeling diode current i_{Dm} decreases linearly. Then,

$$v_x(t) = 0 \tag{10}$$

The commutation interval in this stage is expressed as

$$T_c = \left(\frac{L_r I_o}{V_{in}}\right)[1 - \cos \omega_o (t_2 - t_1)] \tag{11}$$

Notably, the voltage across the power switch Q is zero when the power switch is turned on. It enables the turn-on switching loss to be avoided and the total efficiency of the converter to be increased accordingly.

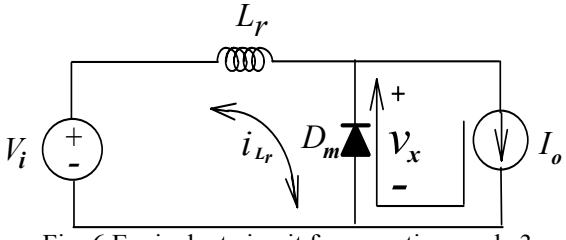

Fig. 6 Equivalent circuit for operating mode 3

Mode 4: (between t_3 and t_4)

When i_{Lr} reaches I_O at t_3, the freewheeling diode D_m is turned off, and the zero-voltage-switched converter resembles a conventional square-wave power processor. The equivalent circuit is shown in Fig. 7.

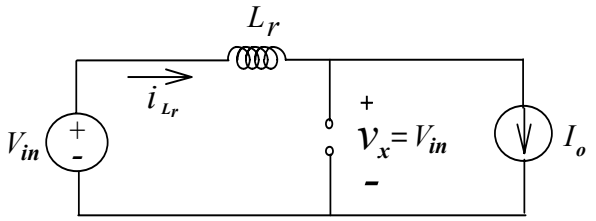

Fig. 7 Equivalent circuit for operating mode 4

The charging current flows through power switch Q and resonant inductor L_r. Accordingly,

$$i_{L_r}(t) = I_o \tag{12}$$

$$v_{C_r}(t) = 0 \tag{13}$$

$$v_x(t) = V_{in} \tag{14}$$

The power switch conducts I_O as long as it is kept on until t_4. At time t_4, the power switch is turned off again and another switching cycle begins. In the above description, the power switch Q and the freewheeling diode D_m in the ZVS converter are commutated under soft-switching. This characteristic makes the ZVS technique particularly appealing for high-frequency conversion applications. Therefore, implementing soft-switching for both the power switch and the freewheeling diode in such a circuit is particularly valuable.

The duration of this mode is T_d, and

$$T_d = T_s - (T_a + T_b + T_c) \tag{15}$$

By controlling the interval T_d of the power switch, the average power supplied to the battery can be controlled.

The output voltage V_{BA} is determined by

$$V_{BA} = V_{in}\left[1 - f_s(t_3 - \frac{t_1}{2})\right] \tag{16}$$

From above equation, it is clear that the charging voltage V_{BA} can be adjusted to desired value by controlling the switching frequency f_S.

Efficiency is an important factor in the battery charger, because it is related with the capacity to injection power in the battery. The power generated by the photovoltaic arrays is

$$P_{pv} = V_{in} I_{pv} \tag{17}$$

The power into the battery is

$$P_{BA} = V_{BA} I_o \tag{18}$$

The efficiency of the battery charger with ZVS converter can be estimated as

$$\eta = \frac{p_{BA}}{P_{pv}} \tag{19}$$

To obtain high efficiency, it is necessary to reduce the switching losses in the charging circuit.

Given I_O and T_S, T_a, T_b and T_c and the output voltage V_{BA} can be determined. However, the voltage conversion ratio is normally best expressed in terms of load resistance R and switching frequency f_S. The output voltage $V_{BA} = rI_o$, so the energy stored in the resonant inductor is

$$E_i = V_{in}\int_{t_1}^{t_2} i_{L_r} dt + V_{in}\int_{t_2}^{t_3} i_{L_r} dt + V_{in} I_o (T_s - t_3 - t_1) \tag{20}$$

The energy released by the low pass filter inductor L_f to the battery is

$$E_o = V_{BA} I_o T_s \tag{21}$$

For a lossless system, these two kinds of energy are equal in the steady state. Hence, the voltage ratio is

$$X = 1 - \frac{f_s}{2\pi f_r}\left[\alpha + \frac{X(1-\cos\alpha)}{r} + \frac{r}{2X}\right] \tag{22}$$

where $X = \frac{V_{BA}}{V_{in}}$ and $\alpha = \omega_0(t_2 - t_1)$ denote the voltage ratio and pulse width angle, respectively.

The relationship between input and output voltages is a function of the pulse width angle, the characteristic impedance of the resonant-switch converter and the output load current. The equation (22) reveals that the output voltage can be controlled by varying the angle for any variation in input voltage and output load current. The voltage ratio of the buck ZVS was numerically determined, as plotted in Fig. 8, with f_s/f_r as the running parameter. Figure 8 plots the dc voltage-conversion-ratio characteristics of the buck ZVS as functions of normalized output current $I_{on} = I_o Z_o / V_{in}$. The first step in designing the converter is to determine f_s/f_r, based on a set of dc characteristics curves for various f_s/f_r .

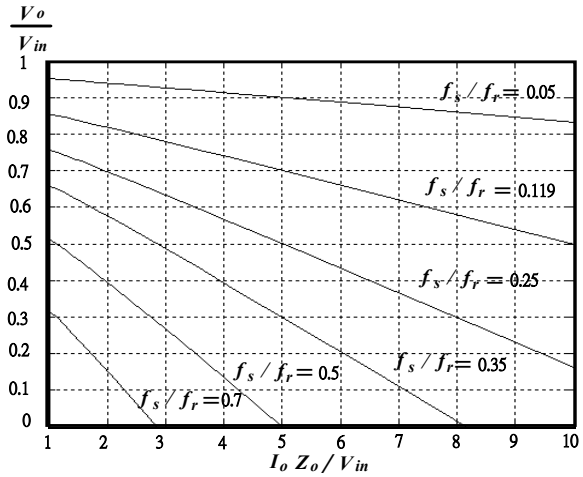

Fig. 8 Conversion ratio for buck ZVS battery charger

The design of the ZVS converter must meet specifications of input voltage, battery voltage, charging current and switching frequency. After the input voltage, the battery voltage, the charging current, and the switching frequency have been chosen, the value of the resonant capacitor is

$$C_r \le \frac{I_o}{V_{in}\omega_r} \tag{20}$$

The inductance is determined from the specifications

$$L_r \ge \frac{V_{in}}{I_o \omega_r} \tag{21}$$

IV. EXPERIMENTAL RESULTS

The input of proposed ZVS was connected to a system consisting of a photovoltaic arrays of output voltage 24V and 75W. A prototype of the buck converter with zero-voltage-switching resonant topology was established in a laboratory to confirm the functional operations. The developed charging circuit is applied to a 12V, 4AH lead-acid battery. The conditions of the experiment were as follows: switching frequency f_S=18KHz, resonant frequency f_r=50KHz, charging current I_O=2A, charging voltage V_{BA} = 15V, and the open circuit voltage of battery V_{OC} =11V. Under these operation conditions, the two parameters of the ZVS converter are chosen as follows:

C_r=0.2μF

L_r=50μH

The waveforms were measured with the help of digital multi-meter. Figure 9 displays the waveforms of the trigger signal V_{GS}, the resonant voltage v_{Cr} and the resonant current i_{Lr}. Figure 10 presents the waveforms of the trigger signal V_{GS} and the voltage v_X during freewheeling period. Fig. 11 plots the waveforms of charging current I_O and resonant current i_{Lr}. Figure 12 displays the voltage variation curve of the charger. The terminal voltage of the battery from 11V to 15V takes 360 minutes. Figures 13 and 14 plot the charging current and the charging efficiency, respectively. The charging current I_O decrease as the voltage V_{BA} of the battery increases. The charging current takes 360 minutes to fall below 0.51A. The minimal and maximal efficiencies of the ZVS charging circuit are around 80% and 87%, respectively, and the mean charging efficiency of the charger is 84%. Under the same operating conditions, the measured temperature of the power switches in the presented battery charger with ZVS resonant converter is maintained at 34℃ and is much lower than that of the traditional PWM converter at 54℃. Fig. 15 shows the measured results for different battery charging converter.

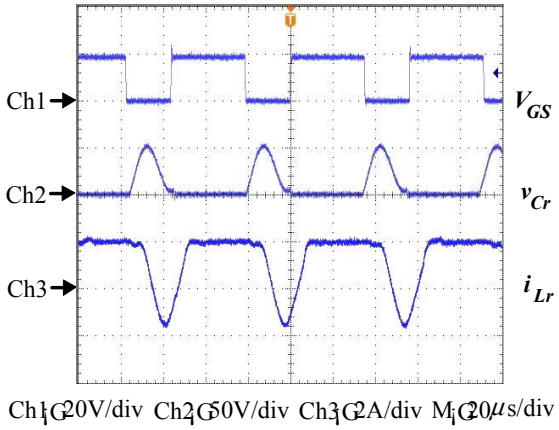

Fig. 9 Waveforms of trigger signal V_{GS}, resonant voltage v_{Cr} and resonant current i_{Lr}

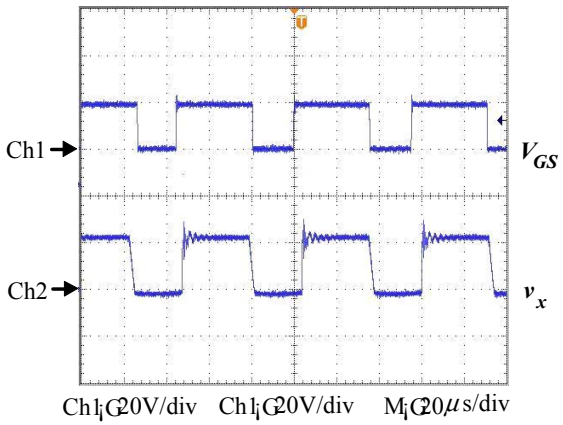

Fig. 10 Waveforms of trigger signal V_{GS} and voltage v_X of freewheeling diode

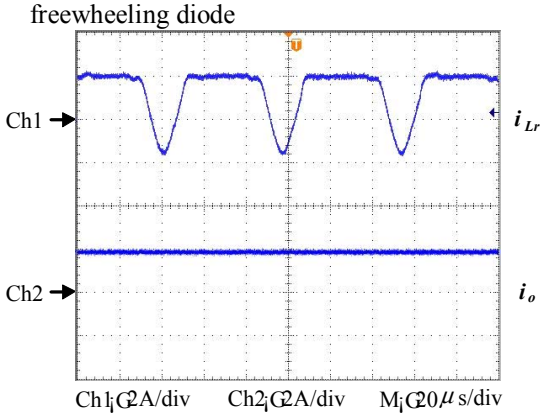

Fig. 11 Waveforms of charging current I_O and resonant current i_{Lr}

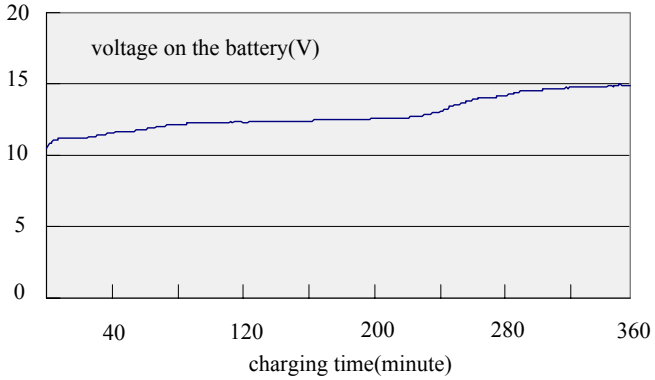

Fig. 12 Battery voltage curve for charging period

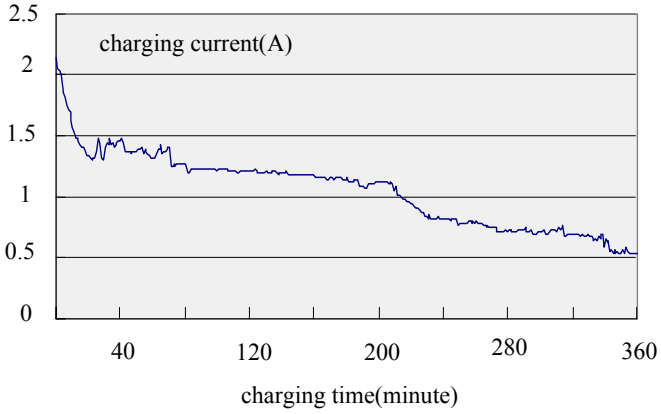

Fig. 13 Charging current curve for charging period

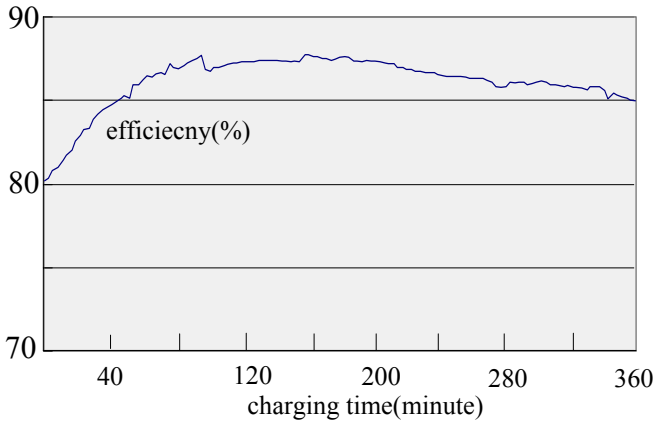

Fig. 14 Charging efficiency curve for charging period

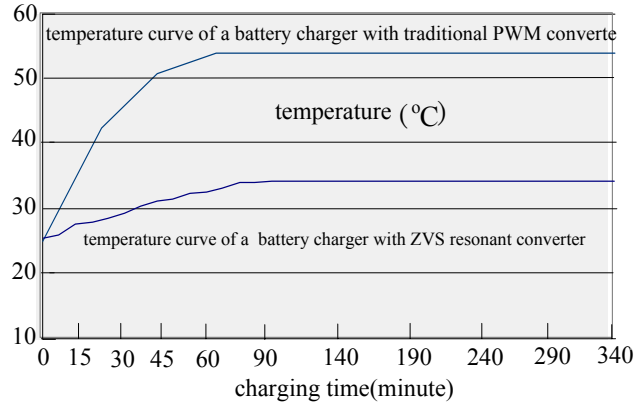

Fig. 15 Comparison of power switch temperatures for different charging circuit

V. CONCLUSIONS

A design of the new battery charger has been proposed for the maximum utilization of the photovoltaic output power. The circuit structure is simpler and much cheaper compared to other control mechanisms where large number of components are needed. This study presents the use of photovoltaic battery charger with ZVS technology in the charging test of a lead-acid battery charger to demonstrate the effectiveness of the developed methodology. Under the same operating conditions, the measured temperature of power switches in the proposed battery charger with ZVS is maintained at 34℃, which is much lower than that of the traditional PWM converter at 54℃. The proposed battery charger with ZVS indeed reduces the temperature of the switch, thus reducing switching losses. The circuit efficiency of the overall charging process exceeds 80% and greatly exceeds the 68% efficiency of traditional PWM converters. Therefore, the charging efficiency can be improved by ZVS technique. Besides, the performance is obtained at lower cost as less number of components are used.

REFERENCES

[1] J. A. Gow and and C. D. Manning, "Photovoltaic Converter System suitable for Use in Small Scale Stand-alone or Grid Connected Applications", IEE Proc. –Electr. Power Appl., Vol. 147, No. 6, pp. 535-543, 2000.

[2] W. A. Tabisz and F. C. Lee, "Zero-Voltage-Switching Multi-Resonant Technique-A Novel Approach to Improve Performance of High Frequency Quasi-Resonant Converters", Power Electronics Specialists Conference, Vol. 19, No. 11-14, pp. 9-17, 1988.

[3] J. G. Cho, J. W. Baek, Geun-Hie Rim, and Iouri Kang, "Novel Zero Voltage Transition PWM Multi-Phase Converters", Applied Power Electronics Conference and Exposition APEC'96 Conference Proceedings Eleventh Annual, Vol. 1, No. 3-7, pp. 500-506, 1996.

[4] Robert W. Erickson, Fundamental of Power Electronics, Second Edition, Kluwer Academic Publishers, 2001.

[5] N. Mohan, T. M. Undeland, and W. P. Robbins, Power Electronics: Converters, Applications and Design, John Wiley & Sons, 3rd Edition, 2003.

[6] A. K. S. Bhat and S. D. Dewan, "Resonant Inverters for Photovoltaic Array to Utility Interface", IEEE Trans. On Aerospace and Electronic Systems, Vol. 24, No. 4, pp. 377-386, 1988.

Ying-Chun Chuang was born in Kaohsiung, Taiwan, R.O.C., in 1962. He received the B. S. Degree in electrical engineering in 1988 from National Taiwan Institute of Technology, Taipei, Taiwan and the M.S. degree in electrical engineering from National Cheng Kung University, Tainan, Taiwan, in 1990 and the Ph.D. degree in electrical engineering from National Yat-Sen University, Kaoshung, Taiwan in 1997. Currently, he is an Associate Professor of the Department of Electrical Engineering, Kun Shan University, Tainan, Taiwan. His research interests are electronic ballasts and power electronic drive systems.

Hung-Shiang Chuang received the M.S. and Ph. D. degrees in mechanical engineering from National Cheng Kung University, Tainan, Taiwan, in 1989 and 2001, respectively. Currently, he is an Associate Professor of the Department of Automation Engineering, Kao Yuan University, Kaohsiung, Taiwan.

Yu-Lung Ke (M'98) was born in Kaohsiung City, Taiwan, on July 13, 1963. He received his B.S. degree in control engineering from National Chiao Tung University, Hsin-Chu City, Taiwan, in 1988. He received his M. S. degree in electrical engineering. from National Taiwan University, Taipei City, Taiwan, in 1991. He received his Ph.D. degree in electrical engineering from National Sun Yat-Sen University, Kaohsiung City, Taiwan, in 2001. Since August 1991, he has been at the Department of Electrical Engineering, Kun Shan University of Technology, Yung-Kang City, Tainan Hsien, Taiwan. He is presently a full Associate Professor.

His research interests include power systems, distribution automation, energy management, power quality, renewable energy and power electronics. Since 2002, Dr. Ke has served as a reviewer for IEEE Transactions on Power Delivery, IEE Proceedings Generation, Transmission and Distribution, International Journal of Electrical Power & Energy Systems and International Journal of Power and Energy Systems. Dr. Ke is a member of IEEE and a registered professional engineer at Taiwan.